Available online at www.sciencedirect.com
ScienceDirect
Trans. Nonferrous Met. Soc. China 24(2014) 3095−3102
Transactions of Nonferrous Metals Society of China
www.tnmsc.cn

Microstructure instability of fully lamellar TiAl alloy containing high content of Nb after long-term thermal cycling

Lu FANG[1], Xian-fei DING[2], Jian-ping HE[1], Lai-qi ZHANG[1], Zhi LIN[1], Jun-pin LIN[1]

1. State Key Laboratory for Advanced Metals and Materials, University of Science and Technology Beijing, Beijing 100083, China;
2. National Center for Materials Service Safety, University of Science and Technology Beijing, Beijing 100083, China

Received 10 October 2013; accepted 20 January 2014

Abstract: Microstructure instabilities of the fully lamellar Ti−45Al−8.5Nb−(W,B,Y) alloy were investigated by SEM and TEM after long-term thermal cycling (500 and 1000 thermal cycles) at 900 °C. Two major categories of microstructure instability were produced in the alloy after the thermal cycling: 1) The discontinuous coarsening implies that grain boundary migrations are inclined to occur in the Al-segregation region after the long-term thermal cycling, especially after 1000 thermal cycles. Al-segregation can be reduced during the process of long-term thermal cycling as a result of element diffusion; 2) The α_2 lamellae become thinner and are broken after 1000 thermal cycles caused by the dissolution of α_2 lamellae through phase transformation of $\alpha_2 \rightarrow \gamma$. The γ grains nucleate within the α_2 lamellae or ($\alpha_2+\gamma$) lamellae in a random direction.

Key words: TiAl alloys; thermal cycling; thermal stability; discontinuous coarsening

1 Introduction

TiAl alloys containing high content of Nb with a fully lamellar structure have been preliminarily applied in fields, such as aerospace and automobile, for their low density, high specific strength, good high-temperature oxidation resistance and creep resistance [1−3]. As the representative of a new generation of high temperature structural materials, the service environment of TiAl alloys containing high content of Nb will be increasingly strict. These alloys work under thermal cycling environment of about 700−1000 °C and different kinds of stress [4,5]. Therefore, long-term stability of the microstructure under service conditions is the major concern in developing TiAl alloys containing high content of Nb before the application.

Currently, many investigations on microstructure instability of TiAl alloys containing high Nb under the service conditions have been carried out [6,7]. These instabilities are manifested as the following three categories [8−10]: 1) phase shape changes and changes of the volume fraction and composition by dissolution/ precipitation of the relevant phases; 2) continuous coarsening by the reduction in interfacial area; 3) discontinuous coarsening by grain boundary migration. In recent studies [5,6,11], especially in long-term thermal exposure, the first two categories were commonly observed but the third one was usually ignored or rarely reported. HUANG et al [6] indicated the microstructure stability of TiAl alloys with high content of Nb during long-term thermal exposure at 700 °C, which includes three types of decomposition of α_2 and γ lamellae. The decomposition of lamellae is driven by the phase equilibria since the ratio of α_2/γ in lamellar structure of original alloys is in nonequilibrium [12]. However, the phenomenon of discontinuous coarsening was not concerned. In addition, in terms of experiment conditions, it is not enough to make studies only on long-term thermal exposure at lower temperature of TiAl alloys containing high Nb. Firstly, the alloys tend to work in thermal cycling environment during the service of

Foundation item: Project (2011CB605500) supported by National Basic Research Program of China; Project (51171015) supported by National Natural Science Foundation of China; Project (2012M520166) supported by China Postdoctoral Science Foundation; Project (2012Z-06) supported by State Key Laboratory for Advanced Metals and Materials, University of Science and Technology Beijing, China; Project (FRF-TP-12-164A) supported by Fundamental Research Funds for the Central Universities of China

Corresponding author: Jun-pin LIN; Tel: +86-10-62332192; E-mail: linjunpin@ ustb.edu.cn

DOI: 10.1016/S1003-6326(14)63447-6

aerospace components. Moreover, the service temperature of TiAl alloys containing high content of Nb is higher than that of conventional TiAl alloys. Some researchers [13,14] have focused on the thermo-mechanical fatigue behavior of TiAl based alloys for a long time. Recently, they announced that loading conditions could reduce fatigue life dramatically compared with the corresponding isothermal conditions. Furthermore, the microstructure instability of TiAl alloys containing high content of Nb induced by long-term thermal cycling may be obviously different because of the production of thermal stress during thermal cycling. However, there are few systematic reports about microstructure instability of TiAl alloy containing high content of Nb during long-term thermal cycling or under thermal cycling creep conditions. Therefore, the studies on microstructure instabilities during long-term thermal cycling are of great importance to service security of TiAl alloys containing high content of Nb. However, the exact regularity of microstructure instability of the alloy during long-term thermal cycling has not been clarified yet.

In this work, the microstructure instabilities after long-term thermal cycling were studied at 900 °C in fully lamellar Ti−45Al−8.5Nb−(W,B,Y) alloy. The forming reasons for the two kinds of microstructure instabilities will be illustrated in detail.

2 Experimental

A fully lamellar cast ingot alloy with a nominal chemical composition of Ti−45Al−8.5Nb−0.2W−0.2B−0.02Y (mole fraction, %) was chosen. In order to obtain the fully lamellar structure, the alloy was heat treated at 1340 °C (in the α-phase field) for 12 h and then transferred to 900 °C for 30 min followed by air cooling.

For thermal cycling tests, the specimens were cut from the alloy using an electro-discharge machine to appropriate dimensions of 12 mm×12 mm×5 mm. The surfaces of the specimens were mechanically polished up to 1200 grit SiC papers and cleaned ultrasonically for 15 min in acetone before thermal cycling test.

Thermal cycling tests were performed from room temperature to 900 °C for 500 and 1000 cycles in a thermal cycling furnace with an auto moving beam (YHL 1.5-12 model). One cycle was composed of holding at 900 °C for 1 h and at ambient temperature for 12 min. The specimens were inserted into and removed from the zone of the furnace within a few seconds to ensure a rapid heating and cooling.

The thermal cycling specimens were polished using standard metallographic techniques. After being teched in the solution of 5 mL HF, 10 mL HNO_3 and 85 mL H_2O, optical microscopy (OM) was used to characterize the lamellar microstructures before the thermal cycling. Microstructural changes were analyzed using a ZEISS SUPRA55 three-dimensional field emission scanning electron microscope (FESEM), equipped with an energy dispersive X-ray spectroscopy (EDS) detector, and a JEM 2010 transmission electron microscope (TEM). Specimens for TEM were prepared by means of twin-jet electro-polishing at 27 V and a temperature of −30 °C.

The mean primary lamellar interface spacing (α_2+γ) was measured by TEM. The α_2 and γ lamellae were tilted 'edge-on'. The measurements were conducted on 30 micrographs that were randomly chosen.

3 Results

3.1 Microstructure before thermal cycling

Figures 1(a) and (b) show the optical and back-scattered electron (BSE) microstructures of the fully lamellar Ti−45Al−8.5Nb−(W,B,Y) alloy before thermal cycling test, respectively. The fully lamellar microstructures are achieved, which are characterized by uniformly distributed fine lamellar colonies (Fig. 1(a)). As shown in Fig. 1(b), the interdendritic dark contrast area exhibits the microsegregation obviously, and the EDS results show that the area is rich in Al and poor in Nb. This shows that the studied alloy solidifies through β-type solidification and the solidification segregation has not been completely removed by the heat treatments.

TEM images in Figs. 2(a) and (b) show the lamellar

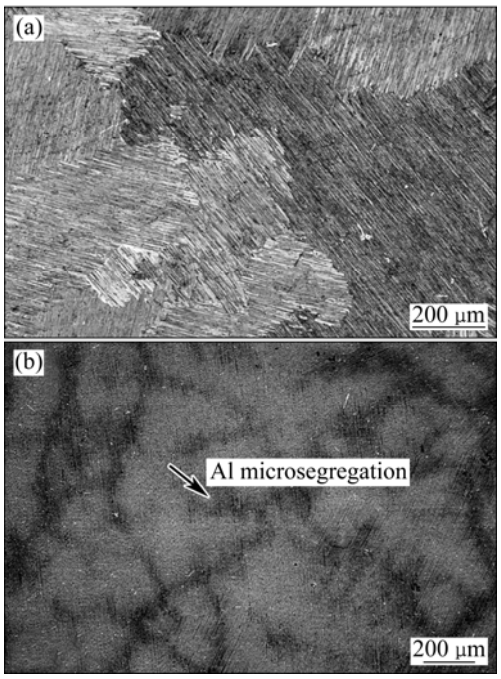

Fig. 1 Optical image (a) and back-scattered electron (BSE) image (b) of fully lamellar Ti−45Al−8.5Nb−(W,B,Y) before thermal cycling tests

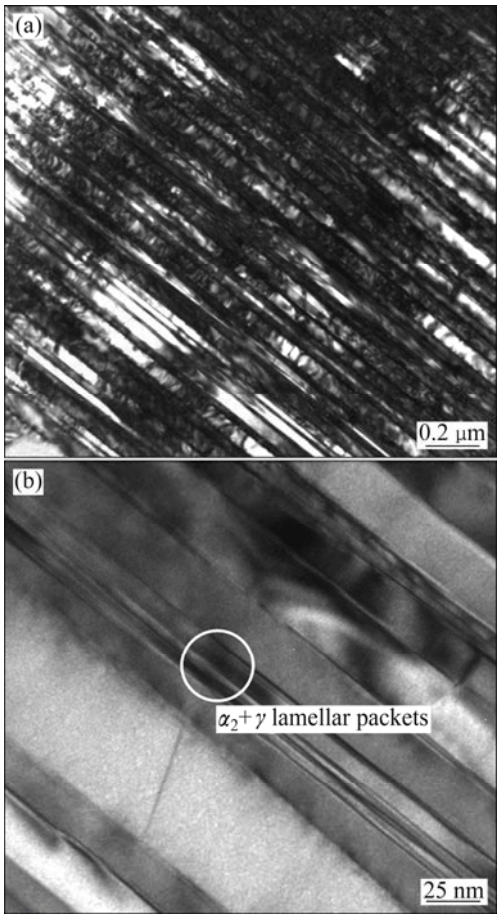

Fig. 2 TEM images of fully lamellar structures in Ti−45Al−8.5Nb−(W,B,Y) alloy: (a) Alternating α_2/γ arrangement; (b) Several finer lamellae in α_2

microstructure in the fully lamellar Ti−45Al−8.5Nb−(W,B,Y) alloy before thermal cycling tests. The lamellar colonies in the original alloy are composed of an alternating arrangement of α_2 (in bright contrast) and γ (in dark contrast). As shown in Fig. 2(b), the interlamellar spacing (63±7 nm) is narrow and some of the lamellar packets between the two γ lamellae are composed of several finer α_2 and γ lamellae.

3.2 Microstructural changes after thermal cycling

Two categories of microstructure instability are observed in the fully lamellar Ti−45Al−8.5Nb−(W,B,Y) alloy after thermal cycling test. They are discontinuous coarsening of primary α_2/γ lamellae occurred in the original Al segregation region and decomposition of α_2 lamellae, and the nucleation of γ grains within the lamellae, respectively.

3.2.1 Discontinuous coarsening (DC) of primary α_2/γ lamellae

Figures 3(a) and (b) separately show the Al microsegregation in Ti−45Al−8.5Nb−(W,B,Y) alloy after 500 and 1000 thermal cycles tests. Compared with the original microstructures in Fig. 1(b), the Al microsegregation can be reduced notably due to the element diffusion during the long-term thermal cycling. Figures 3(c) and (d) show the enlarged views of the lamellar microstructures in Al-segregation region of the alloy after 500 and 1000 thermal cycles, respectively. The areas of Al microsegregation still consist of lamellar colony. As shown in Fig. 3(c), the lamellar

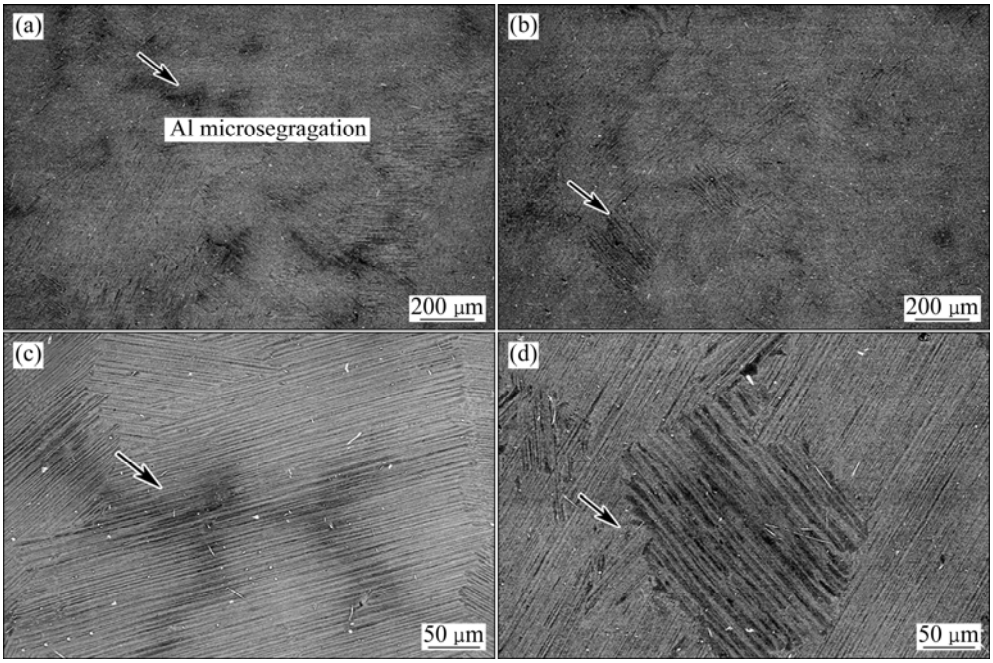

Fig. 3 SEM images of Ti−45Al−8.5Nb−(W,B,Y) alloy after long-term thermal cycling: (a) Al microsegregation after 500 thermal cycles; (b) Al microsegregation after 1000 thermal cycles; (c) Lamellae in Al-segregation region after 500 thermal cycles; (d) Lamellae in Al-segregation region after 1000 thermal cycles

microstructure in the Al-segregation area almost unchanges as compared with that in other regions after 500 thermal cycles. However, after 1000 thermal cycles, the interlamellar spacing increases obviously in the Al-segregation region and most of the lamellar orientations in the coarsening region are different from the original primary lamellae. This suggests that discontinuous coarsening should generate in interdendritic region [8,15]. Table 1 lists the EDS analysis result of discontinuous coarsening lamellae and primary lamellae regions in the alloy after 1000 thermal cycles. The Al content in discontinuous coarsening (DC) lamellae is higher than that in the primary lamellae.

Table 1 EDS compositions of discontinuous coarsening (DC) lamellae and primary lamellae regions in alloy after 1000 thermal cycles

Sample	Mole fraction/%		
	Ti	Al	Nb
DC lamellae	43.42(±0.16)	48.25(±0.21)	8.32(±0.05)
Primary lamellae	44.37(±0.17)	47.17(±0.20)	8.46(±0.05)

Figure 4 shows the EPMA mapping result image of the discontinuous coarsening lamellar (in left side) and primary lamellar (in right side) microstructure. The percentage of Al element in the left side is evidently higher than that in the right side, which is consistent with the EDS data. Moreover, no precipitated phase has been found along grain boundary.

Figures 5(a) and (b) show the phenomenon of discontinuous coarsening in the studied TiAl alloy after 1000 thermal cycles tests. Figure 5(a) shows the morphology of discontinuous coarsening which is formed along the colony boundary where the coarsened lamellae are nearly perpendicular to the colony boundary. Figure 5(b) shows another kind of morphology of the discontinuous coarsening. It is formed along the colony boundary where the coarsened lamellae on one side of the colony boundary are nearly perpendicular to the colony boundary, but the coarsened lamellae on the other side of the colony boundary are nearly parallel to the colony boundary. Both types have been mentioned in TiAl alloys without Nb addition [15,16] which are called as type I and type II. The discontinuous coarsening microstructures, as shown in Figs. 5(a) and (b), are both coarser lamellar structure and still consist of α_2 and γ. However, little type III discontinuous coarsening can be found in the alloy which contains tortuous secondary lamellae. This lamellae have no obvious orientation of the colony boundary with the primary lamellae on both sides of the boundary. It may be because of the lower driving force at the lower temperature (900 °C) [15].

Figures 6(a) and (b) show the discontinuous coarsening indicated by white circle. It can be clearly seen that not only the interlamellar spacing but also the

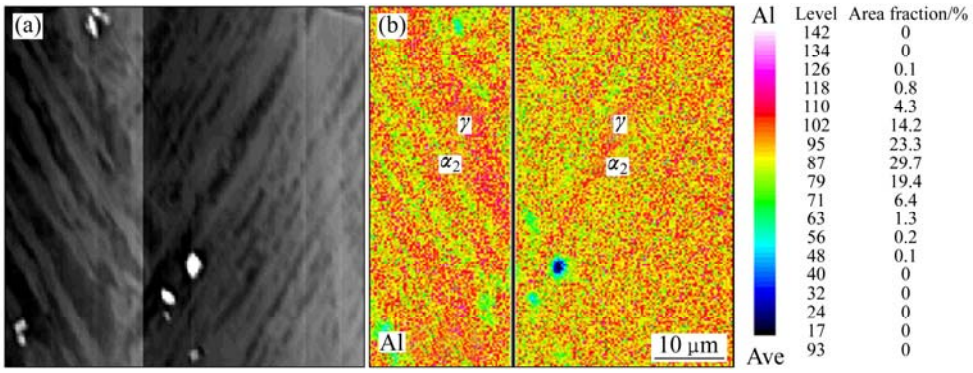

Fig. 4 SEM image (a) and EPMA mapping results (b) of discontinuous coarsening lamellae (in left side) and primary lamellae (in right side) microstructure

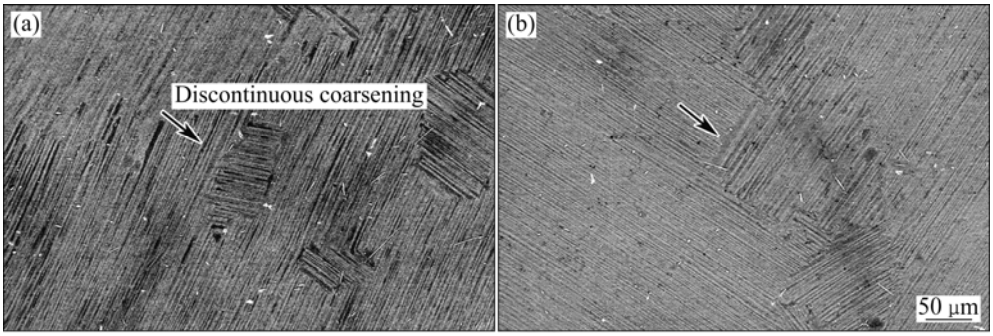

Fig. 5 Discontinuous coarsening of α_2/γ in alloy after 1000 thermal cycles: (a) Type I; (b) Type II

lamellar thickness of discontinuous coarsening lamellae are much larger than those of primary lamellae. The degree of discontinuous coarsening is different which could be the reason for the difference of lamellar thicknesses in Figs. 6(a) and (b) (indicated by white circle). And the residual primary α_2/γ lamellae (indicated by arrow) should be the evidence for the formation of discontinuous coarsening by consuming its primary α_2/γ lamellae.

3.2.2 Decomposition of α_2 lamellae and nucleation of γ grains

Figures 7(a)−(d) show TEM images of the microstructures after 1000 thermal cycles. The corresponding images of the microstructures after 500 thermal cycles are not shown here, for the microstructure changes of the alloy after 500 thermal cycles are not apparent yet compared with 1000 thermal cycles. From Fig. 7, α_2 lamellae become thinner due to the dissolution

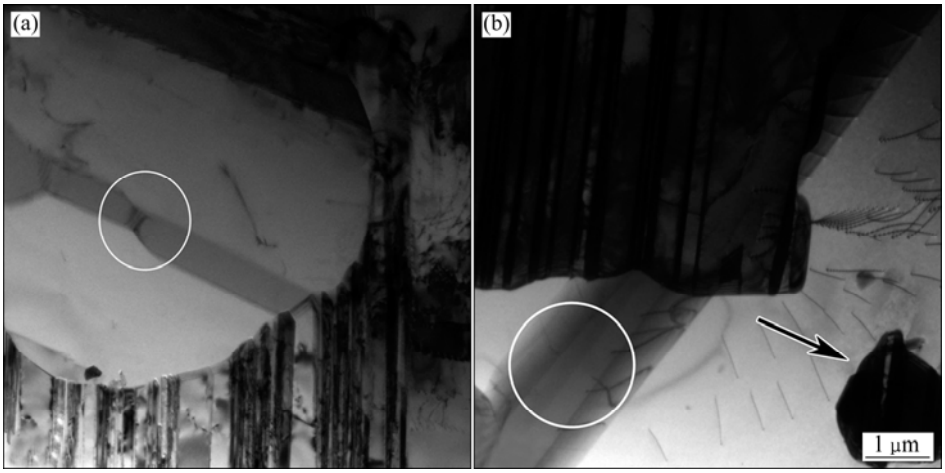

Fig. 6 TEM images of discontinuous coarsening with different lamellar thicknesses in Ti−45Al−8.5Nb−(W,B,Y) alloys

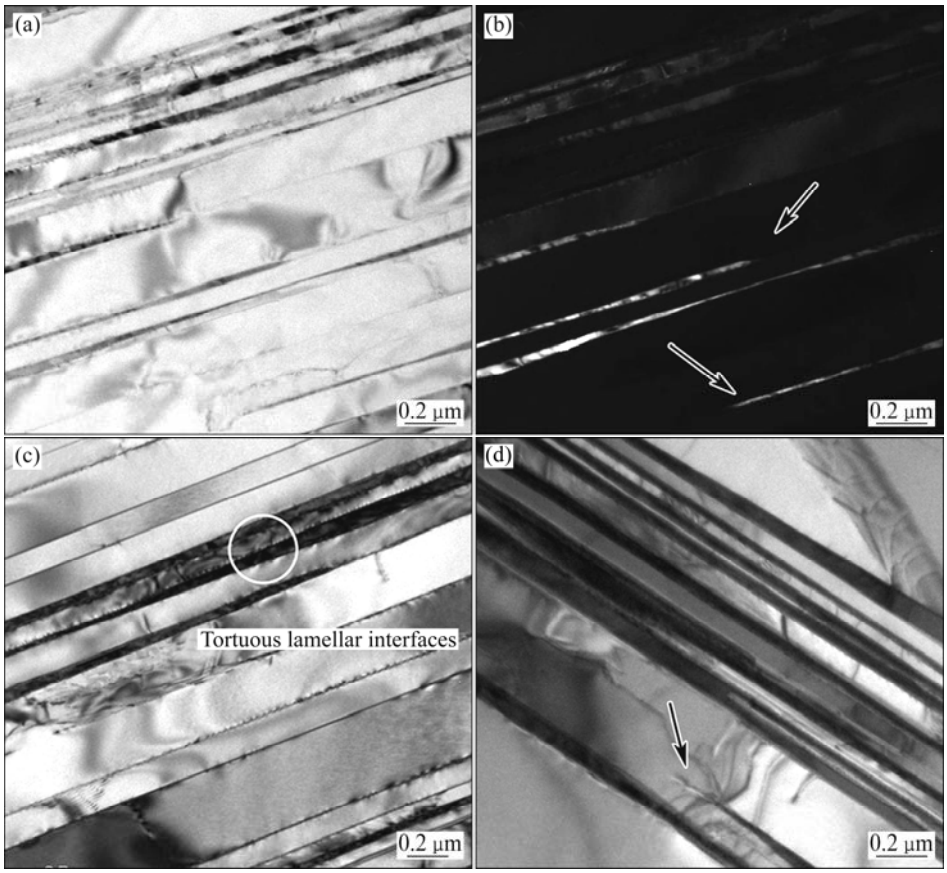

Fig. 7 TEM images of microstructures after 1000 thermal cycles of decomposition of α_2 lamellae occurring between adjacent γ laths: (a) Bright field; (b) Corresponding dark field images; (c) γ/γ interface compared with original microstructure and tortuous lamellar interfaces; (d) Dislocations emission at top of broken α_2 laths

of α_2 through phase transformation $\alpha_2 \rightarrow \gamma$ (indicated by the arrow). Moreover, compared with the original microstructure (Fig. 2(a)), there is an increasing number of γ/γ interfaces because of the complete decomposition of α_2 between adjacent γ laths (Fig. 7(c)).

Furthermore, tortuous lamellar interfaces (Fig. 7(c)) and broken α_2 laths (Figs. 7(a)−(d)) can be observed in the TEM images. And the dislocations emission often appears on the top of broken α_2 laths (Fig. 7(d)).

The nucleation of γ grains (Figs. 8(a) and (b)) in a random direction (confirmed by the diffraction patterns) within the α_2 lamellae or ($\alpha_2+\gamma$) lamellar structure is also observed after 1000 thermal cycles, which was also reported by HUANG et al [17] and BESCHLIESSER et al [11] after long-term thermal exposure.

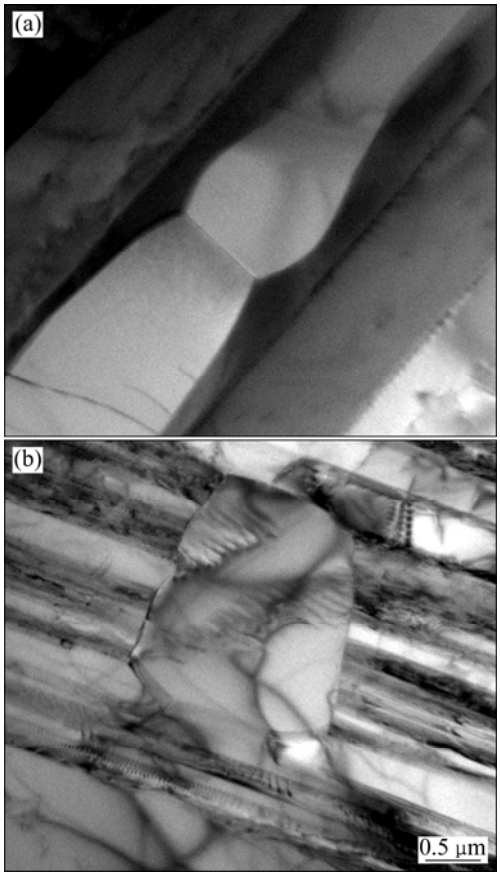

Fig. 8 TEM images of lamellar microstructures after 1000 thermal cycles: (a) Nucleation of γ grains in a random direction within α_2 lamellae; (b) Nucleation of γ grains in a random direction within ($\alpha_2+\gamma$) lamellae

4 Discussion

The experimental results clearly reveal the two categories of microstructure instability observed in fully lamellar TiAl alloy containing high Nb after long-term thermal cycling. They are discontinuous coarsening of primary α_2/γ lamellae occurred in the original Al segregation region and decomposition of α_2 lamellae through phase transformation $\alpha_2 \rightarrow \gamma$ and nucleation of γ grains within the lamellae, respectively. The following discussions will mainly focus on the discontinuous coarsening, because the other one has been discussed in detail in many references.

Discontinuous coarsening is generated from boundary moving reaction which needs no change in crystal structure, but involves only compositional adjustment. The driving force for discontinuous coarsening is mainly from the reduction of interface energy and chemical free energy [18]. As shown in Figs. 1 and 2, the narrow primary interlamellar spacing means that the interface formation energy of the α_2/γ lamellae should be high. Moreover, the volume fraction and chemical fraction of the α_2 and γ are far away from the equilibrium state. Driven by the chemical free energy, Ti and Al atom can be redistributed through the long-term thermal cycling at 900 °C. However, it is generally known that the semicoherent interface of α_2/γ which follows the Blackburn orientation relationship $\{111\}_\gamma // \{0001\}_{\alpha_2}$ and $<11\bar{2}0>_{\alpha_2} // <110>_\gamma$ has the low energy [16,19]. It is difficult for the element to diffuse through α_2/γ interface. Therefore, the grain boundary becomes the main channel for element diffusion. In conclusion, it is likely to produce the large driving force, the reduction of interface energy and chemical free energy, which benefits the formation of discontinuous coarsening (Fig. 5). The discontinuous coarsening with large interlamellar spacing is formed with consuming its primary α_2/γ lamellae [19].

Nevertheless, it was documented that the discontinuous coarsening phenomenon in TiAl alloys often occurs above 900 °C because the increase of interface free energy with increasing heat-treatment temperature will easily lead to the formation of discontinuous coarsening [16]. This may be the reason why the phenomenon of discontinuous coarsening was not found in the TiAl alloys during long-term thermal exposure below 900 °C [6,12]. However, in this work, under the long-term thermal cycling conditions, the alloy was heated and cooled between 900 °C and room temperature, in which the internal stresses could be produced caused by the thermal mismatch of elastic modulus and thermal expansion between α_2 and γ phase [5]. Therefore, this process leads to the generation of a lot of interface free energy between the α_2 and γ phase. In other words, this process leads to the generation of a great deal of energy which might be the driving force of the discontinuous coarsening. In addition, with increasing number of cycles, the volume fraction of discontinuous coarsening increases.

With regard to the preference sites of discontinuous coarsening, EDS compositions analysis in Table 1 and EPMA result in Fig. 4 indicate that discontinuous

coarsening is inclined to occur in the Al-segregation region. The reason is that the thickness of γ lamellae is larger than that of α_2 lamellae in discontinuous coarsening lamellae, which is more obvious than in the primary lamellae. Namely, interdiffusion of Al element should be one of the prerequisites to discontinuous coarsening, which could also illustrates the importance of chemical driving force for discontinuous coarsening from another aspect.

In general, the overall driving force ΔG_{DC} per unit volume of a discontinuous coarsening reaction can be expressed as follows [18]:

$$\Delta G_{DC} = \Delta G_{DC}^{c} + \Delta G_{DC}^{\gamma} = \Delta G_{DC}^{c} + \left(\frac{2\gamma V_m}{\lambda_{DC}} - \frac{2\gamma V_m}{\lambda_0} \right) \quad (1)$$

where ΔG_{DC}^{c} and ΔG_{DC}^{γ} are the reduction of chemical free energy and the reduction of α_2/γ interface energy in unit volume before and after the discontinuous coarsening reaction, respectively; V_m is the molar volume of alloy; λ_{DC} and λ_0 are the interlamellar spacing in primary lamellae and discontinuous coarsening lamellae, respectively. As a result, the driving force for discontinuous coarsening increases with the decrease of λ_0. Moreover, it should be noted that long-term thermal cycling would provide larger driving force than long-term thermal exposure at the same temperature, because a great deal of extra α_2/γ interface free energy is generated during long-term thermal cycling due to the internal stresses caused by the thermal mismatch of elastic modulus and thermal expansion between α_2 and γ phases.

As to the decomposition of α_2 lamellae, it is driven by the phase equilibria because the volume fraction of the γ phase is lower than that at equilibrium. In addition, with narrower interlamellar spacing, the phase nonequilibria increases and the dissolution of α_2 lamellae becomes more serious (Fig. 7). Figure 8 shows γ grains, which grow into (α_2+γ) lamellae or nucleate within α_2 lamellae. This process is driven by fault and edge migration. More detailed information about the mechanisms of the process have been given in Refs. [8,11,17].

5 Conclusions

1) The interdiffusion of Al element should be one of the prerequisites to discontinuous coarsening.

2) The long-term thermal cycling would provide larger driving force of discontinuous coarsening than long-term thermal exposure at the same temperature, because a great deal of extra α_2/γ interface free energy is generated during long-term thermal cycling.

3) The α_2 lamellae become thinner and broke after 1000 thermal cycles, which is driven by the phase equilibria because the volume fraction of the γ phase is lower than that at equilibrium.

References

[1] KIM Y W. Gamma titanium aluminides: Their status and future [J]. JOM, 1995, 47(7): 39−42.

[2] MARKETZ W T, FISCHER F D, CLEMENS H. Deformation mechanisms in TiAl intermetallics—Experiments and modeling [J]. International Journal of Plasticity, 2003, 19(3): 281−321.

[3] KIM Y W. Intermetallic alloys based on gamma titanium aluminide [J]. JOM, 1989, 41(7): 24−30.

[4] FRITZ A, ULRICH B, ULRICH C, STEFAN E, PETER J, UWE L, JOHANN M, MICHAEL O, PAUL J D H. Recent progress in the development of gamma titanium aluminide alloys [J]. Advanced Engineering Materials, 2000, 2(11): 699−720.

[5] ZHAO W Y, PEI Y L, ZHANG D H, MA Y, GONG S K, XU H B. The microstructure and tensile property degradation of a gamma-TiAl alloy during isothermal and cyclic high temperature exposures [J]. Intermetallics, 2011, 19(3): 429−432.

[6] HUANG Z W, VOICE W, BOWEN P. Thermal exposure induced $\alpha_2+\gamma\rightarrow$B2($\omega$) and $\alpha_2\rightarrow$B2(ω) phase transformations in a high Nb fully lamellar TiAl alloy [J]. Scripta Materialia, 2003, 48(1): 79−84.

[7] BYSTRZANOWSKI S, BARTELS A, CLEMENS H, GERLING R, SCHIMANSKY F P, DEHM G, KESTLER H. Creep behaviour and related high temperature microstructural stability of Ti−46Al−9Nb sheet material [J]. Intermetallics, 2005, 13(5): 515−524.

[8] RAMANUJAN R V, MAZIASZ P J, LIU C T. The thermal stability of the microstructure of γ-based titanium aluminides [J]. Acta Materialia, 1996, 44(7): 2611−2642.

[9] SHARMA G, RAMANUJAN R V, TIWARI G P. Instability mechanisms in lamellar microstructures [J]. Acta Materialia, 2000, 48(4): 875−889.

[10] DENQUIN A, NAKA S. Phase transformation mechanisms involved in two-phase TiAl-based alloys—II. Discontinuous coarsening and massive-type transformation [J]. Acta Materialia, 1996, 44(1): 353−365.

[11] BESCHLIESSER M, CHATTERJEE A, LORICH A, KNABL W, KESTLER H, DEHM G, CLEMENS H. Designed fully lamellar microstructures in a γ-TiAl based alloy: Adjustment and microstructural changes upon long-term isothermal exposure at 700 and 800 °C [J]. Materials Science and Engineering A, 2002, 329: 124−129.

[12] CHENG T T. Effects of thermal exposure on the microstructure and properties of a γ-TiAl based alloy containing 44Al−4Nb−4Zr−0.2Si−0.3B [J]. Intermetallics, 1999, 7(9): 995−999.

[13] BAUER V, CHRIST H J, Thermomechanical fatigue behaviour of a third generation γ-TiAl intermetallic alloy [J]. Intermetallics, 2009, 17(5): 370−377.

[14] XIANG H F, DAI A L, WANG J H, LI H, YANG R. Cyclic deformation behaviors of Ti−46Al−2Cr−2Nb−0.15B alloy during thermo-mechanical fatigue tests [J]. Transactions of Nonferrous Metals Society of China, 2010, 20(11): 2174−2180.

[15] TANG J C, HUANG B Y, HE Y H, XIE K. Morphology of discontinuous coarsening in fully lamellar TiAl [J]. Transactions of Nonferrous Metals Sociefy of China, 2000, 10(1): 10−13.

[16] MITAO S, BENDERSKY L A. Morphology and growth kinetics of discontinuous coarsening in fully lamellar Ti−44 Al (at.%) alloy [J]. Acta Materialia, 1997, 45(11): 4475−4489.

[17] HUANG Z W, VOICE W, BOWEN P. The effects of long-term air exposure on the stability of lamellar TiAl alloys [J]. Intermetallics, 2000, 8(4): 417−426.
[18] MANNA I, PABI S K, GUST W. Discontinuous reactions in solids [J]. International Materials Reviews, 2001, 46(2): 53−91.
[19] QIN G, WANG J, HAO S. Discontinuous coarsening of primary α_2/γ lamellae at colony boundaries in γ-TiAl-based alloys [J]. Intermetallics, 1999, 7(1): 1−4.

全片层高 Nb 含量 TiAl 合金长期热循环后的显微组织不稳定性

方 璐[1]，丁贤飞[2]，何建平[1]，张来启[1]，林 志[1]，林均品[1]

1. 北京科技大学 新金属材料国家重点实验室，北京 100083；
2. 北京科技大学 国家材料服役安全科学中心，北京 100083

摘 要：对全片层 Ti−45Al−8.5Nb−(W,B,Y)合金在 900 ℃下进行长期热循环(500 次和 1000 次)实验，采用扫描电镜(SEM)及透射电镜(TEM)研究该合金长期热循环后的显微组织不稳定性。结果表明：合金经热循环后主要产生两种类型的组织不稳定性：1) 长期热循环特别是 1000 次热循环后，在 Al 偏析处易产生因晶界迁移引起的不连续粗化，随着循环次数的增加，元素扩散致使 Al 偏析逐渐减少；2) 1000 次热循环后，α_2 片层变细且发生断裂，这是由 $\alpha_2 \rightarrow \gamma$ 相变导致的 α_2 片层溶解所致。同时，γ 晶粒在 α_2 片层或($\alpha_2+\gamma$)片层内部以任意方向形核。

关键词：TiAl 合金；热循环；热稳定性；不连续粗化

(Edited by Chao WANG)